Supporting Information

Foster et al. 10.1073/pnas.0900729106

SI Materials and Methods

Materials. All reagents were from Sigma unless otherwise noted. Diethylamine NONOate was from Cayman Chemicals. *S*-nitrosocysteine and *S*-nitrosoglutathione were synthesized by mixing equimolar volumes of $NaNO_2$/1 mM EDTA in deionized water with thiol in 0.5 M HCl. For synthesis of *S*-nitroso-4-mercaptophenylacetic acid, the thiol was dissolved in isopropanol containing 0.5 M HCl. After mixing with $NaNO_2$, PASNO was immediately neutralized with NaOH and diluted further with HEN buffer [250 mM Hepes, 1 mM EDTA, 0.1 mM neocuproine (pH 7.7)]. Protoarray Yeast and Human Proteome Microarrays for KSI were from Invitrogen. ORF-overexpressing yeast were from Open Biosystems. Mouse anti-HA and anti-Flag M2 antibodies were from Sigma–Aldrich. Rabbit anti-Cdk5 was from Santa Cruz Biotechnology, and rabbit anti-MK2 was from Cell Signaling Technology.

Detection of Protein *S*-Nitrosylation on Protein Microarrays. Incubations were performed in slide chambers unless otherwise noted. Buffers were filtered (0.22 μm) before use. Invitrogen Protoarrays for kinase substrate identification (KSI) were first blocked by rocking with 10 mM lysine in PBS for 4 h at 4 °C. After several washes with PBS, where noted, proteins were reduced with 5 mM DTT in PBS for 30 min at 4 °C. Pretreatment with DTT did not substantially alter the pattern of *S*-nitrosylation, indicating that neither adventitious oxidation nor endogenous protein disulfides are major limitations. Slides were washed with PBS to remove DTT and finally with 250 mM Hepes, 1 mM EDTA, 0.1 mM neocuproine (pH 7.4) (HEN 7.4). After removal of excess buffer, 300 μL of HEN 7.4 (with or without nitrosothiols) was pipetted onto the slides. A Hybrislip (60 mm × 22 mm; Molecular Probes) was placed on top of the solution, and slides were incubated in the dark for 30 min. Next, slides were washed once with HEN buffer (pH 7.7) and placed in a slide chamber with the same buffer containing 20 mM methyl methanethiosulfonate (MMTS) and 1% SDS. Slide chambers were incubated, vertically, in the dark for 20 min in a 50 °C water bath for blocking of free thiols. To remove excess MMTS, slides were washed four times with a 10-fold dilution of HEN buffer and finally with HEN buffer. Finally, proteins were biotinylated by incubating slides for 1 h in the dark with HEN buffer containing 5 or 50 mM ascorbate, 0.4 mM biotin-HPDP, and 1% SDS by using a Hybrislip as described above.

After the biotinylation step, slides were washed liberally with PBS containing 0.05% Tween-20 (PBST) and further blocked with 1% BSA in PBST for 2 h at 4 °C. Slides were incubated with 1:500 anti-biotin-M antibody (Vector) in PBST overnight at 4 °C. After washing PBST (3 times for 10 min), slides were incubated with 1:1,000 Alexa Fluor 647-labeled goat anti-mouse secondary antibody (Molecular Probes) in PBST for 1 h at room temperature. Finally, slides were washed with PBST (3 times for 10 min) and once with PBS. Slides were placed in 50-mL conical flasks and dried by centrifugation in a swinging bucket rotor at 700 × *g* for 5 min. Slides were scanned and with a Genepix 4000b scanner (Molecular Devices) using Genepix Pro and analyzed by using Prospector Analyzer (Invitrogen). SNO-proteins were identified by visual inspection and by comparing background-subtracted mean fluorescence intensities for each spot compared to buffer-treated controls.

Cloning and Purification of Yeast Proteins. His-tagged Qns1p was expressed and purified from *E. coli* by using the plasmid pB337 (kindly provided by C. Brenner, University of Iowa) (1). For all other proteins, yeast ORFs were amplified from *S. cerevisiae* genomic DNA (Novagen) by PCR (see Table S4 for list of primers) and cloned into pET-15b, pET-21b, or PGEX-2TK. C116S Ych1p was generated by using the QuikChange site-directed mutagenesis kit (Stratagene). Proteins were expressed in Rosetta 2(DE3)pLysS *E. coli*. His-tagged proteins were expressed in LB and induced at O.D. ≈0.6–1 for 4 h under the following optimized conditions (growth temperature, induction temperature, [IPTG]): Arl1p, Arf1p, Hsp31p and Yuh1p (37 °C, 37 °C, 0.5 mM); Rdl1p and Rdl2p (30 °C, 30 °C, 0.1 mM); wild-type and C116S Ych1p(30 °C, 25°C, 0.1 mM). Additionally, GST-Uba4 was grown at 30°C to O.D. ≈1.0 and induced with 0.5 mM IPTG overnight at room temperature. For purification of His-tagged proteins, cell pellets were lysed by sonication in 20 mM Tris, 150 mM NaCl, 20 mM imidazole, 1 mM PMSF (pH 8.0). After centrifugation, lysates were incubated with Ni-NTA Agarose (Qiagen) for 1 h, washed with lysis buffer containing 500 mM NaCl, and eluted with lysis buffer containing 250 mM imidazole. For purification of Arl1p and Arf1p, all buffers contained 2 mM $MgCl_2$ and 100 μM GDP. Mg- or MgGDP-free proteins were prepared by extensive buffer exchange (with buffer containing 5 mM EDTA). For purification of GST-Uba4p, cells were lysed in 20 mM Tris, 500 mM NaCl, 1 mM EDTA, 2 mM DTT (pH 8.0) and lysates were incubated with glutathione-Sepharose for 1 h at 4 °C. After washing with lysis buffer, protein was eluted with 200 mM Tris, 15 mM GSH (pH 8.0). Typically, purified proteins were exchanged into 25 mM Tris, 150 mM NaCl, 1 mM EDTA (pH 7.4) and stored at −20 °C. Because of its precipitation and inactivation after free-thawing, GST-Uba4p was kept on ice and used within 48 h of purification.

***S*-Nitrosylation Assays.** The biotin switch assay was performed on purified proteins as described previously (2). SNOs were quantified by using Hg-coupled photolysis chemiluminescence (3). Excess NO donors were removed by desalting on Biogel P-6 (Bio-Rad) or by repeated spin concentration/dilution using Amicon Ultra 10-kDa centrifugal filters (Millipore). SNO-sites were mapped on Uba4p as described previously (4). Briefly, purified GST-Uba4p (2 mg/mL; ≈0.25 μM) was treated with 0.5 mM CysNO for 15 min followed by desalting. After blocking of free thiols and desalting twice with Biogel P-6, *S*-nitrosylated Cys residues were labeled with biotin-HPDP in the presence of 25 mM ascorbate, and Uba4p was precipitated to remove excess biotin-HPDP and solubilized in buffer containing 1% SDS. Uba4p was extensively dialyzed against 50 mM ammonium bicarbonate and digested overnight with 1:50 trypsin at 37 °C. Biotinylated peptides were purified over monomeric avidin and eluted with 40% aqueous acetonitrile containing 0.1% TFA. Peptides were identified at the Duke Proteomics Core Facility by LC-MS/MS and MASCOT searches against the yeast proteome with variable modifications for biotinylated Cys (+428).

Rhodanese and Phosphatase Assays. For assay of rhodanese activity, 3 μL of protein (10 μM Rdl2p, 100 μM Rdl1p, or 100 μM Uba4p) was added to 87 μL of reaction buffer [0.1 M Tris (pH 7.5) containing 10 mM KCN and 0.1 mM EDTA]. Ten microliters of 500 mM sodium thiosulfate was added, and after 5 min at 37 °C, the reaction was stopped by addition of 50 μL of 15% formaldehyde and thiocyanate was visualized by addition of 150 μL of iron reagent as previously described (5). After dilution to 500 μL with water, $FeSCN^-$ was measured at 460 nm. To assay

inhibition of Rdl2p, protein was first pretreated with reaction buffer for 10 min at room temperature and desalted, to ensure that the protein was not in the persulfide-bound form.

For measurement of phosphatase activity, 10 μL of 3-*O*-methylfluorescein phosphate (OMFP; 5 mg/mL in PBS) was added to 1 μM Ych1p in 100 mM Tris, 0.1 mM EDTA (pH 7.5), and the formation of 3-*O*-methylfluorescein was measured continuously at 490 nm for 5 min at room temperature. For treatments with H_2O_2, 10 μM enzyme was reacted with H_2O_2 for 5 min followed by 10-fold dilution of the enzyme to 1 μM into 125 units of catalase before addition of OMFP.

NAD$^+$ Synthetase Assay. One microgram of Qns1p in 44 μL of assay buffer [50 mM Tris (pH 8.0) containing 0.1 mM EDTA, 1 mM $NaAD^+$, 2 mM ATP, 5 mM $MgCl_2$, 56 mM KCl (1)] was incubated with 1 μL of inhibitor (DON) or *S*-nitrosothiol for 30 min at 30 °C, followed by addition of 5 μL of 0.2 M glutamine. After incubating at 37 °C for 10 min, the reaction was quenched by adding 200 μL of 7 M NaOH. After heating at 95 °C for 5 min, the amount of NAD^+ formed was measured by fluorescence (ex. 390 nm, em. 460 nm) as described previously (6).

Ubiquitin Hydrolase Assay. Yuh1p (1 μM) in 50 mM Tris, 0.1 mM EDTA (pH 7.5) was treated with *S*-nitrosothiol for 15 min followed by dilution to 1 nM in the same buffer. Yuh1p (1 nM, 10 μL) was added to 90 μL of 500 pM ubiquitin-AMC (Biomol). Formation of fluorescent AMC was measured continuously for 10 min (ex. 380 nm; em. 460 nm).

1. Bieganowski P, Pace HC, Brenner C (2003) Eukaryotic NAD+ synthetase Qns1 contains an essential, obligate intramolecular thiol glutamine amidotransferase domain related to nitrilase. *J Biol Chem* 278:33049–33055.
2. Foster MW, Stamler JS (2004) New insights into protein *S*-nitrosylation. Mitochondria as a model system. *J Biol Chem* 279:25891–25897.
3. Stamler JS, et al. (1992) Nitric oxide circulates in mammalian plasma primarily as an *S*-nitroso adduct of serum albumin. *Proc Natl Acad Sci USA* 89:7674–7677.
4. Whalen EJ, et al. (2007) Regulation of beta-adrenergic receptor signaling by *S*-nitrosylation of G-protein-coupled receptor kinase 2. *Cell* 129:511–522.
5. Williams RA, Kelly SM, Mottram JC, Coombs GH (2003) 3-Mercaptopyruvate sulfurtransferase of *Leishmania* contains an unusual C-terminal extension and is involved in thioredoxin and antioxidant metabolism. *J Biol Chem* 278:1480–1486.
6. Zalkin H (1985) NAD synthetase. *Methods Enzymol* 113:297–302.
7. *Saccharomyces* Genome Database, www.yeastgenome.org.
8. Pace HC, Brenner C (2001) The nitrilase superfamily: Classification, structure and function. *Genome Biol* 2: REVIEWS0001.
9. Baker RT, Varshavsky A (1995) Yeast N-terminal amidase. A new enzyme and component of the N-end rule pathway. *J Biol Chem* 270:12065–12074.
10. Lefievre L, et al. (2007) Human spermatozoa contain multiple targets for protein S-nitrosylation: An alternative mechanism of the modulation of sperm function by nitric oxide? *Proteomics* 7:3066–3084.
11. AbdelRaheim SR, Cartwright JL, Gasmi L, McLennan AG (2001) The NADH diphosphatase encoded by the *Saccharomyces cerevisiae* NPY1 nudix hydrolase gene is located in peroxisomes. *Arch Biochem Biophys* 388:18–24.
12. Abid R, Ueda K, Miyazaki M (1997) Novel features of the functional site and expression of the yeast deoxyhypusine synthase. *Biol Signals* 6:157–165.
13. Stephens CM, Bauerle R (1992) Essential cysteines in 3-deoxy-D-arabino-heptulosonate-7-phosphate synthase from *Escherichia coli*. Analysis by chemical modification and site-directed mutagenesis of the phenylalanine-sensitive isozyme. *J Biol Chem* 267:5762–5767.
14. Hartmann M, et al. (2003) Evolution of feedback-inhibited beta/alpha barrel isoenzymes by gene duplication and a single mutation. *Proc Natl Acad Sci USA* 100:862–867.
15. Schnappauf G, Hartmann M, Kunzler M, Braus GH (1998) The two 3-deoxy-D-arabino-heptulosonate-7-phosphate synthase isoenzymes from *Saccharomyces cerevisiae* show different kinetic modes of inhibition. *Arch Microbiol* 169:517–524.
16. Branson JP, Nezic M, Jitrapakdee S, Wallace JC, Attwood PV (2004) Kinetic characterization of yeast pyruvate carboxylase isozyme Pyc1 and the Pyc1 mutant, C249A. *Biochemistry* 43:1075–1081.
17. Mathieu M, et al. (1997) The 1.8 A crystal structure of the dimeric peroxisomal 3-ketoacyl-CoA thiolase of *Saccharomyces cerevisiae*: Implications for substrate binding and reaction mechanism. *J Mol Biol* 273:714–728.
18. Joseph E, Wei W, Tittmann K, Jordan F (2006) Function of a conserved loop of the beta-domain, not involved in thiamin diphosphate binding, in catalysis and substrate activation in yeast pyruvate decarboxylase. *Biochemistry* 45:13517–13527.
19. Le Moan N, Clement G, Le Maout S, Tacnet F, Toledano MB (2006) The *Saccharomyces cerevisiae* proteome of oxidized protein thiols: Contrasted functions for the thioredoxin and glutathione pathways. *J Biol Chem* 281:10420–10430.
20. Heurgue-Hamard V, et al. (2006) The zinc finger protein Ynr046w is plurifunctional and a component of the eRF1 methyltransferase in yeast. *J Biol Chem* 281:36140–36148.
21. Yamaguchi T, et al. (1998) ADP-ribosylation factor-1 is sensitive to N-ethylmaleimide. *J Biochem* 124:1229–1236.
22. Schmitz J, et al. (2008) The sulfurtransferase activity of Uba4 presents a link between ubiquitin-like protein conjugation and activation of sulfur carrier proteins. *Biochemistry* 47:6479–6489.
23. Furukawa K, Mizushima N, Noda T, Ohsumi Y (2000) A protein conjugation system in yeast with homology to biosynthetic enzyme reaction of prokaryotes. *J Biol Chem* 275:7462–7465.
24. Tauler A, Bartrons R, Pons G, Carreras J (1983) Metabolism of glycerate-2,3-P2–IV. Effect of Hg2+ on the enzymes involved in the metabolism of glycerate-2,3-P2 in pig skeletal muscle. *Comp Biochem Physiol B* 76:789–793.
25. Gonzalez E, et al. (2000) Characterization of a (2R,3R)-2,3-butanediol dehydrogenase as the *Saccharomyces cerevisiae* YAL060W gene product. Disruption and induction of the gene. *J Biol Chem* 275:35876–35885.
26. Gonzalez E, Fernandez MR, Larroy C, Pares X, Biosca JA (2001) Characterization and functional role of *Saccharomyces cerevisiae* 2,3-butanediol dehydrogenase. *Chem Biol Interact* 130–132:425–434.
27. Street IP, Coffman HR, Baker JA, Poulter CD (1994) Identification of Cys139 and Glu207 as catalytically important groups in the active site of isopentenyl diphosphate:dimethylallyl diphosphate isomerase. *Biochemistry* 33:4212–4217.
28. Li X, et al. (2006) Crystal structure of 3-hydroxyanthranilic acid 3,4-dioxygenase from *Saccharomyces cerevisiae*: A special subgroup of the type III extradiol dioxygenases. *Protein Sci* 15:761–773.
29. Niessing D, Huttelmaier S, Zenklusen D, Singer RH, Burley SK (2004) She2p is a novel RNA binding protein with a basic helical hairpin motif. *Cell* 119:491–502.
30. Quevillon-Cheruel S, et al. (2006) Crystal structure of the yeast His6 enzyme suggests a reaction mechanism. *Protein Sci* 15:1516–1521.
31. Ghezzi P, et al. (2006) Redox regulation of cyclophilin A by glutathionylation. *Proteomics* 6:817–825.
32. Greco TM, et al. (2006) Identification of *S*-nitrosylation motifs by site-specific mapping of the *S*-nitrosocysteine proteome in human vascular smooth muscle cells. *Proc Natl Acad Sci USA* 103:7420–7425.
33. Demasi M, Silva GM, Netto LE (2003) 20 S proteasome from *Saccharomyces cerevisiae* is responsive to redox modifications and is *S*-glutathionylated. *J Biol Chem* 278:679–685.
34. Arndt JW, et al. (2005) Crystal structure of an alpha/beta serine hydrolase (YDR428C) from *Saccharomyces cerevisiae* at 1.85 A resolution. *Proteins* 58:755–758.
35. Netz DJ, Pierik AJ, Stumpfig M, Muhlenhoff U, Lill R (2007) The Cfd1-Nbp35 complex acts as a scaffold for iron-sulfur protein assembly in the yeast cytosol. *Nat Chem Biol* 3:278–286.
36. Nakshatri H, Bhat-Nakshatri P, Currie RA (1996) Subunit association and DNA binding activity of the heterotrimeric transcription factor NF-Y is regulated by cellular redox. *J Biol Chem* 271:28784–28791.
37. Senger B, Despons L, Walter P, Jakubowski H, Fasiolo F (2001) Yeast cytoplasmic and mitochondrial methionyl-tRNA synthetases: Two structural frameworks for identical functions. *J Mol Biol* 311:205–216.
38. Curran SP, et al. (2004) The role of Hot13p and redox chemistry in the mitochondrial TIM22 import pathway. *J Biol Chem* 279:43744–43751.
39. Ckless K, et al. (2004) In situ detection and visualization of *S*-nitrosylated proteins following chemical derivatization: identification of Ran GTPase as a target for *S*-nitrosylation. *Nitric Oxide* 11:216–227.
40. Ho YS, Burden LM, Hurley JH (2000) Structure of the GAF domain, a ubiquitous signaling motif and a new class of cyclic GMP receptor. *EMBO J* 19:5288–5299.
41. Li YF, Hess S, Pannell LK, White Tabor C, Tabor H (2001) In vivo mechanism-based inactivation of *S*-adenosylmethionine decarboxylases from *Escherichia coli*, *Salmonella typhimurium*, and *Saccharomyces cerevisiae*. *Proc Natl Acad Sci USA* 98:10578–10583.
42. Sirkis R, Gerst JE, Fass D (2006) Ddi1, a eukaryotic protein with the retroviral protease fold. *J Mol Biol* 364:376–387.
43. Amor JC, et al. (2001) Structures of yeast ARF2 and ARL1: Distinct roles for the N terminus in the structure and function of ARF family GTPases. *J Biol Chem* 276:42477–42484.
44. Lu L, Hong W (2003) Interaction of Arl1-GTP with GRIP domains recruits autoantigens Golgin-97 and Golgin-245/p230 onto the Golgi. *Mol Biol Cell* 14:3767–3781.
45. Qiu C, Lienhard S, Hynes NE, Badache A, Leahy DJ (2008) Memo is homologous to nonheme iron dioxygenases and binds an ErbB2-derived phosphopeptide in its vestigial active site. *J Biol Chem* 283:2734–2740.
46. Meier M, Janosik M, Kery V, Kraus JP, Burkhard P (2001) Structure of human cystathionine beta-synthase: A unique pyridoxal 5′-phosphate-dependent heme protein. *EMBO J* 20:3910–3916.
47. Dong YX, Sueda S, Nikawa J, Kondo H (2004) Characterization of the products of the genes SNO1 and SNZ1 involved in pyridoxine synthesis in *Saccharomyces cerevisiae*. *Eur J Biochem* 271:745–752.
48. Forsee WT, McPherson D, Schutzbach JS (1997) Characterization of recombinant yeast dolichyl mannosyl phosphate synthase and site-directed mutagenesis of its cysteine residues. *Eur J Biochem* 244:953–958.
49. Krautwurst H, et al. (1995) *Saccharomyces cerevisiae* phosphoenolpyruvate carboxykinase: Revised amino acid sequence, site-directed mutagenesis, and microenvironment characteristics of cysteines 365 and 458. *Biochemistry* 34:6382–6388.

50. Alvear M, Encinas MV, Kemp RG, Latshaw SP, Cardemil E (1992) ATP-dependent *Saccharomyces cerevisiae* phospho enol pyruvate carboxykinase: Isolation and sequence of a peptide containing a highly reactive cysteine. *Biochim Biophys Acta* 1119:35–38.
51. Veal EA, et al. (2004) A 2-Cys peroxiredoxin regulates peroxide-induced oxidation and activation of a stress-activated MAP kinase. *Mol Cell* 15:129–139.
52. Cronk JD, Endrizzi JA, Cronk MR, O'Neill JW, Zhang KY (2001) Crystal structure of *E. coli* beta-carbonic anhydrase, an enzyme with an unusual pH-dependent activity. *Protein Sci* 10:911–922.
53. Taylor SC, Ferguson AD, Bergeron JJ, Thomas DY (2004) The ER protein folding sensor UDP-glucose glycoprotein-glucosyltransferase modifies substrates distant to local changes in glycoprotein conformation. *Nat Struct Mol Biol* 11:128–134.
54. Nakaseko Y, Neuhaus D, Klug A, Rhodes D (1992) Adjacent zinc-finger motifs in multiple zinc-finger peptides from SWI5 form structurally independent, flexibly linked domains. *J Mol Biol* 228:619–636.
55. Heo J, Campbell SL (2005) Mechanism of redox-mediated guanine nucleotide exchange on redox-active Rho GTPases. *J Biol Chem* 280:31003–31010.
56. Allen S, Lu H, Thornton D, Tokatlidis K (2003) Juxtaposition of the two distal CX3C motifs via intrachain disulfide bonding is essential for the folding of Tim10. *J Biol Chem* 278:38505–38513.
57. Lu H, Woodburn J (2005) Zinc binding stabilizes mitochondrial Tim10 in a reduced and import-competent state kinetically. *J Mol Biol* 353:897–910.
58. Kumaran D, Eswaramoorthy S, Studier FW, Swaminathan S (2005) Structure and mechanism of ADP-ribose-1′-monophosphatase (Appr-1′-pase), a ubiquitous cellular processing enzyme. *Protein Sci* 14:719–726.
59. Hu RG, Wang H, Xia Z, Varshavsky A (2008) The N-end rule pathway is a sensor of heme. *Proc Natl Acad Sci USA* 105:76–81.
60. Li J, Pickart CM (1995) Binding of phenylarsenoxide to Arg-tRNA protein transferase is independent of vicinal thiols. *Biochemistry* 34:15829–15837.
61. Jaffrey SR, Erdjument-Bromage H, Ferris CD, Tempst P, Snyder SH (2001) Protein *S*-nitrosylation: A physiological signal for neuronal nitric oxide. *Nat Cell Biol* 3:193–197.
62. Kelleher ZT, Matsumoto A, Stamler JS, Marshall HE (2007) NOS2 regulation of NF-kappaB by *S*-nitrosylation of p65. *J Biol Chem* 282:30667–30672.
63. Forrester MT, et al. (2009) Proteomic analysis of *S*-nitrosylation and denitrosylation by resin-assisted capture. *Nat Biotechnol* 27:557–559.
64. Sayed N, Baskaran P, Ma X, van den Akker F, Beuve A (2007) Desensitization of soluble guanylyl cyclase, the NO receptor, by *S*-nitrosylation. *Proc Natl Acad Sci USA* 104:12312–12317.
65. Kwiecien I, Sokolowska M, Luchter-Wasylewska E, Wlodek L (2003) Inhibition of the catalytic activity of rhodanese by *S*-nitrosylation using nitric oxide donors. *Int J Biochem Cell Biol* 35:1645–1657.
66. Spallarossa A, et al. (2003) Inhibition of *Azotobacter vinelandii* rhodanese by NO-donors. *Biochem Biophys Res Commun* 306:1002–1007.
67. Tomko RJ, Jr, Lazo JS (2008) Multimodal control of Cdc25A by nitrosative stress. *Cancer Res* 68:7457–7465.
68. Pi X, Wu Y, Ferguson JE, III, Portbury AL, Patterson C (2009) SDF-1alpha stimulates JNK3 activity via eNOS-dependent nitrosylation of MKP7 to enhance endothelial migration. *Proc Natl Acad Sci USA* 106:5675–5680.
69. Xian M, et al. (2000) Inhibition of protein tyrosine phosphatases by low-molecular-weight *S*-nitrosothiols and *S*-nitrosylated human serum albumin. *Biochem Biophys Res Commun* 268:310–314.
70. Chen YY, et al. (2008) Cysteine *S*-nitrosylation protects protein-tyrosine phosphatase 1B against oxidation-induced permanent inactivation. *J Biol Chem* 283:35265–35272.
71. Carver DJ, Gaston B, Deronde K, Palmer LA (2007) Akt-mediated activation of HIF-1 in pulmonary vascular endothelial cells by *S*-nitrosoglutathione. *Am J Resp Cell Mol Biol* 37:255–263.
72. Barrett DM, et al. (2005) Inhibition of protein-tyrosine phosphatases by mild oxidative stresses is dependent on *S*-nitrosylation. *J Biol Chem* 280:14453–14461.
73. Braun O, Knipp M, Chesnov S, Vasak M (2007) Specific reactions of *S*-nitrosothiols with cysteine hydrolases: A comparative study between dimethylargininase-1 and CTP synthetase. *Protein Sci* 16:1522–1534.
74. Xian M, Chen X, Liu Z, Wang K, Wang PG (2000) Inhibition of papain by *S*-nitrosothiols. Formation of mixed disulfides. *J Biol Chem* 275:20467–20473.
75. Venturini G, Colasanti M, Salvati L, Gradoni L, Ascenzi P (2000) Nitric oxide inhibits falcipain, the *Plasmodium falciparum* trophozoite cysteine protease. *Biochem Biophys Res Commun* 267:190–193.

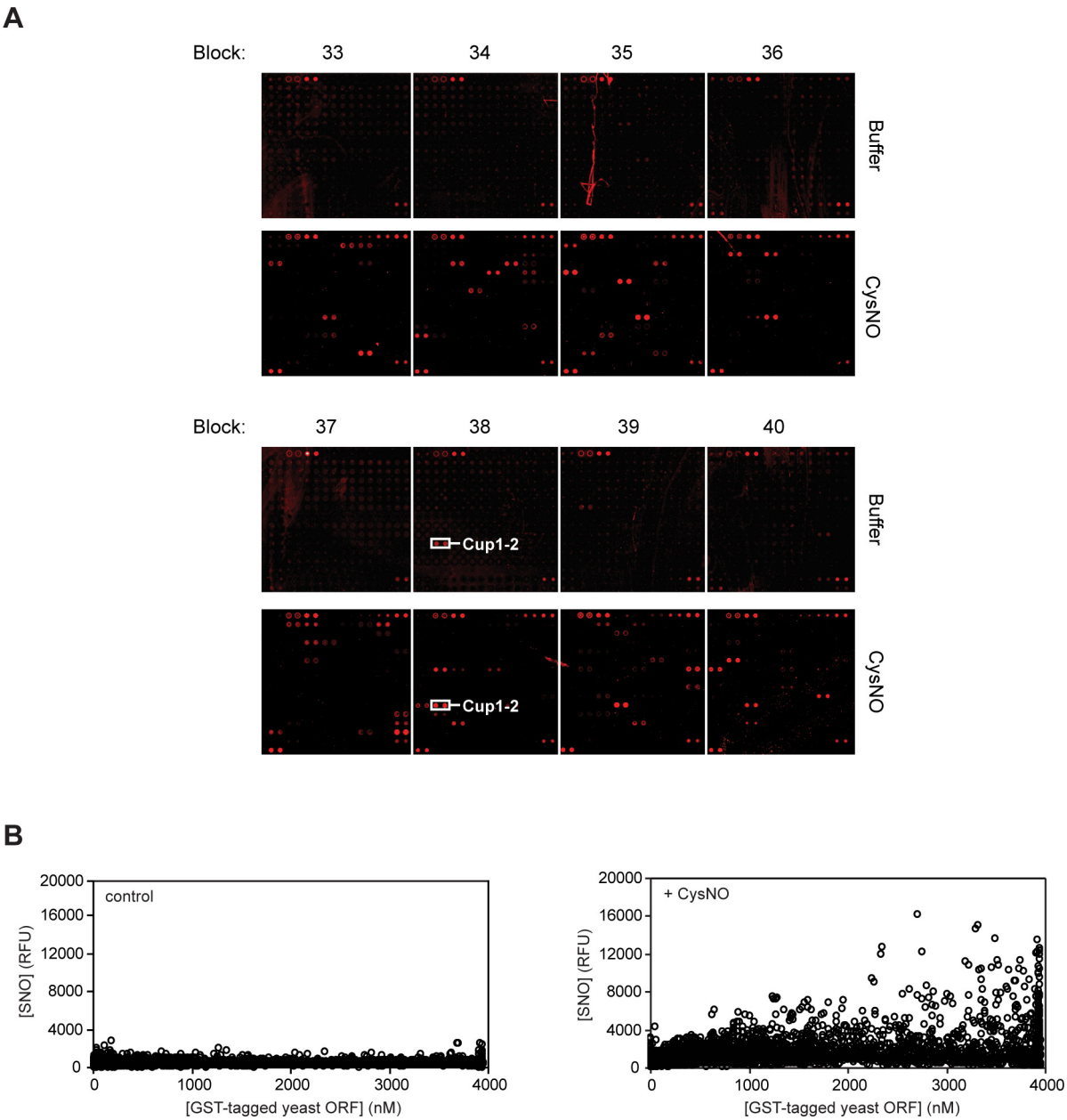

Fig. S1. Detection of *S*-nitrosylation on protein microarrays. A modified BST (see *Materials and Methods*) was applied to yeast Protoarrays that were exposed either to buffer alone or 50 μM CysNO for 30 min. (*A*) Eight blocks (nos. 33–40) are shown for each condition. The locations of positive and negative controls are as in Fig. 1. Very few proteins gave substantial labeling on the untreated slide. One exception (red box; block 38) was Yhr055cp (Cup1–2p), a metallothionein with 20% Cys content (12 of 61 amino acids), which is indicative of incomplete blocking. Images are representative of at least three independent experiments. (*B*) Slides were scanned, and the background-subtracted mean fluorescence intensities for each spot were quantified. These values were plotted against protein concentrations (supplied by Invitrogen) obtained by probing slides with anti-GST antibody.

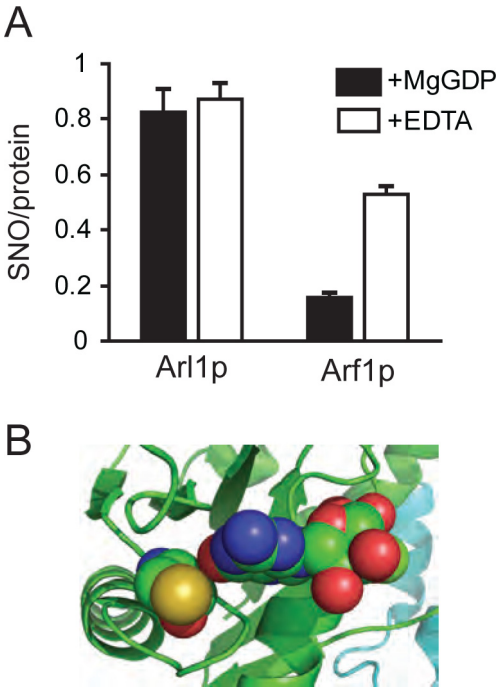

Fig. S2. *S*-nitrosylation of Arf1p and Arfl1p GTPases. (*A*) MgGDP-bound Arl1p- and Arf1pΔ17-MgGDP (1 μM) was treated with 50 μM CySNO for 15 min, and after desalting, *S*-nitrosylation was quantified by Hg-coupled photolysis-chemiluminescence after treatment of the proteins with a 50-fold excess of CysNO for 15 min. To test effect of nucleotide removal on Arf1p *S*-nitrosylation, proteins were treated with 5 mM EDTA, which facilitates nucleotide exchange from GTPases lacking the N-terminal amphipathic helix. Data are mean ± SEM. ($n = 3$). (*B*) Structure of Mg-GDP-bound Arf1p (PDBID code 1RE0) showing proximity of target Cys thiol (*Left*; sulfur atom shown in yellow) to the guanine base (*Right*).

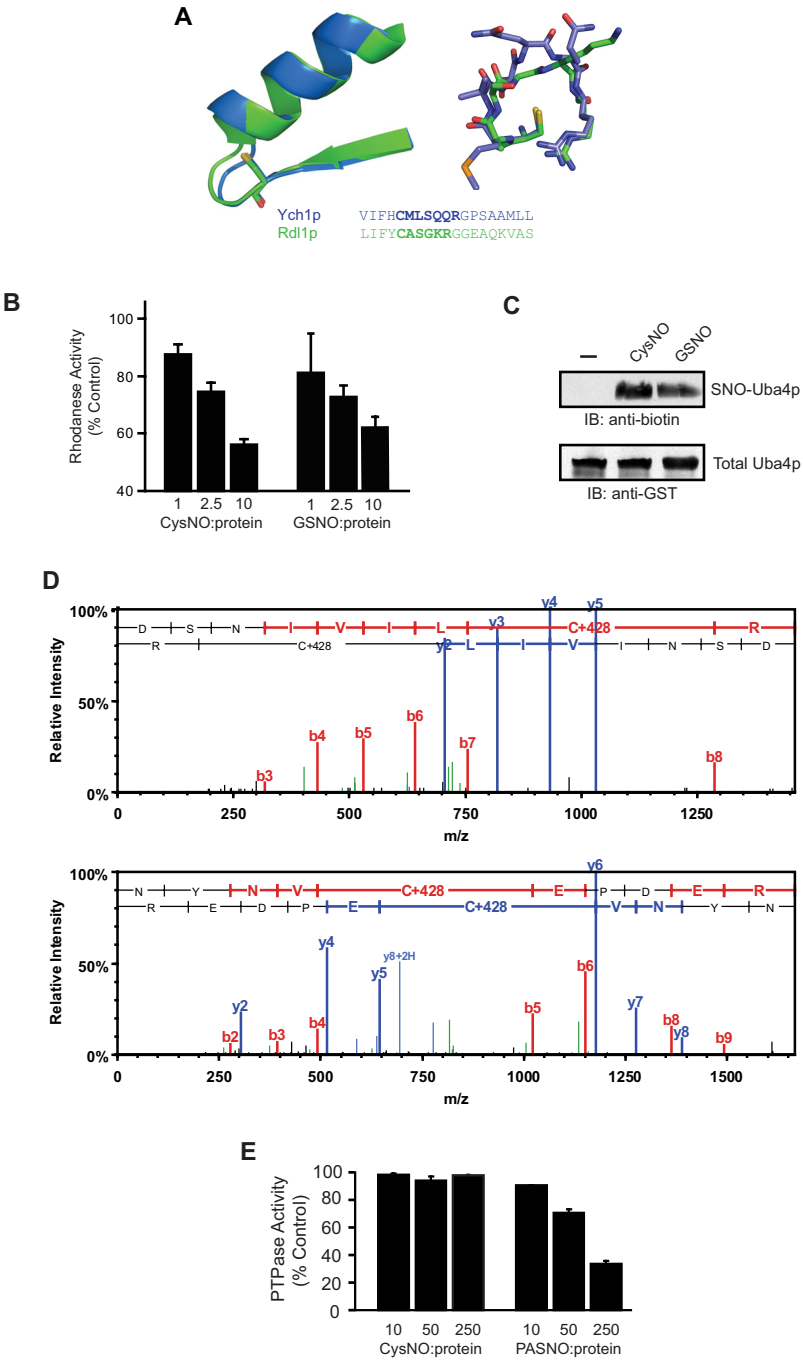

Fig. S3. Structure of rodanese/Cdc25 phosphatase and cysteines hydrolase active-site folds. (*A*) The protein backbones (*Left*) and catalytic loops (*Right*) of the yeast phosphatase Ych1p (PDB ID code 3F4A; blue) and rhodanese Rdl1p (PDB ID code 3D1P; green) were aligned. Despite low sequence homology (see sequence alignment; catalytic loops are in bold), the protein backbones are nearly superimposable in this region. Note that the position of the N-terminal Cys and C-terminal Arg of the catalytic loops are in similar positions, with the Cys thiol protruding from the center of the catalytic pocket; however, the Ych1p catalytic loop contains 6 amino acids (vs. 5 for Rdl1p) and the positions of the side chains between the Cys and Arg vary greatly between the two structures. Alignments were performed and structures generated by using Pymol. (*B*) Rhodanese activity was measured after incubation of Uba4 (100 μM) with the indicated molar ratios of SNO:protein for 10 min. (*C*) Uba4 (10 μM) was treated with 50 μM CysNO or GSNO for 15 min and analyzed by the BST. (*D*) MS/MS spectra of biotinylated Cys peptides that were recovered after trypsin digestion of SNO-treated and BST-analyzed Uba4p. The tryptic peptide DSNIVILCR (upper spectrum) contains to the rhodanese active-site Cys. (*E*) C116S Ych1p (1 μM) was treated with the indicated molar ratios of CysNO or PASNO for 10 min and phosphatase activity was assayed as described in *SI Materials and Methods*. Data in *B* and *E* are mean ($n = 3$) $\pm$ SEM. Images in *C* are representative of two independent experiments.

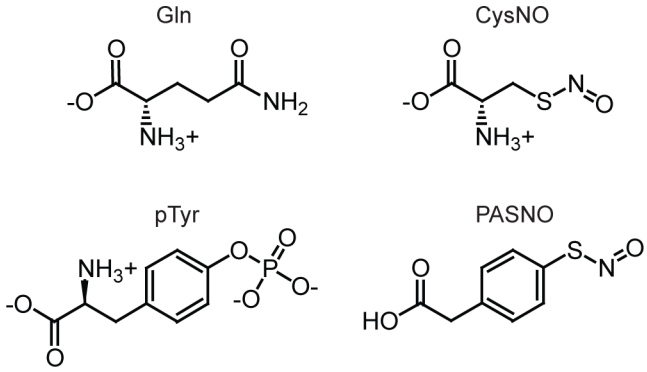

Fig. S4. Structures of enzyme substrates and their *S*-nitrosothiol mimetics. The structures of phosphotyrosine (pTyr) and glutamine (Gln) are shown in comparison with PASNO and CysNO.

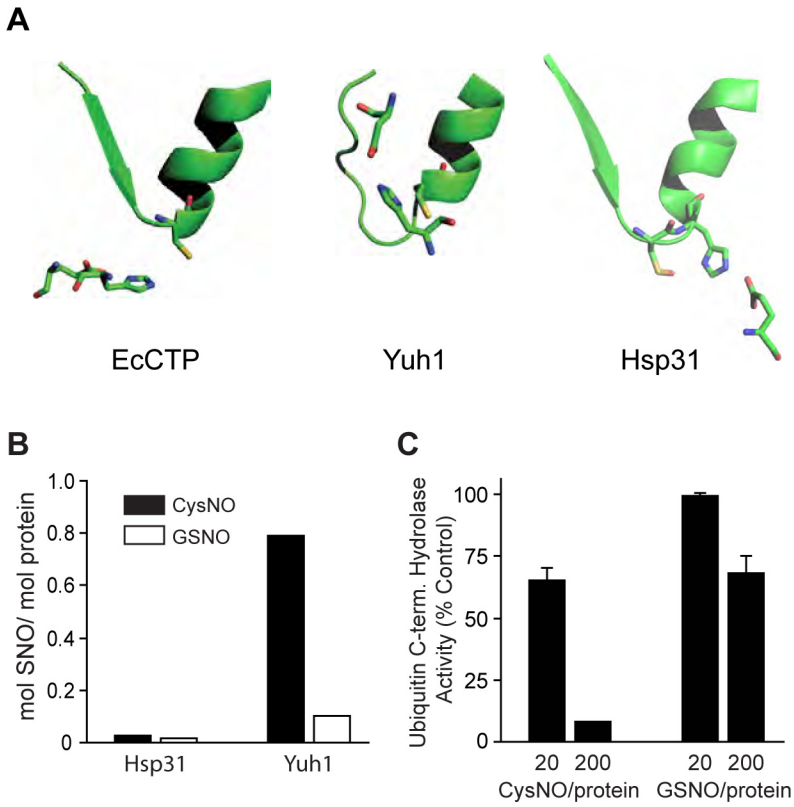

Fig. S5. Structure and reactivity of Cys-dependent hydrolases. (*A*) Nucleophilic elbow motifs, with (putative) catalytic triad residues (Cys, His, Asp/Glu) are shown for exemplary GAT domain, DUB, and Hsp31/DJ-1 family members, *E. coli* CTP synthetase (PDB ID code 1S1M), Yuh1p (PDB ID code 1CMX) and yeast Hsp31p (PDB ID code 1QVZ). Note that in the structure of Yuh1p, the catalytic Cys is covalently bound to ubiquitin aldehyde, and in the structure of Hsp31p, the active-site Cys is oxidized. Structures were generated by using Pymol. (*B*) Hsp31p and Yuh1p (1 μM) were incubated with 50 μM CysNO or GSNO for 15 min and after desalting, *S*-nitrosylation was quantified by photolysis-chemiluminescence. (*C*) Yuh1p (1 μM) was incubated with SNOs for 15 min, and the activity of 1 nM enzyme was assessed by using 0.5 μM ubiquitin-AMC. Data in *B* are mean ($n = 3$) and data in *C* are mean $\pm$ SEM.

Other Supporting Information

Table S1
Table S2
Table S3
Table S4